J Control Theory Appl 2011 9 (1) 3–9
DOI 10.1007/s11768-011-0236-7

Body sensor networks for ubiquitous healthcare

Shaofeng WANG, Lianying JI, Aiguang LI, Jiankang WU
Sensor Networks and Applications Research Center, Graduate University and Institute of Automation,
Chinese Academy of Sciences, Beijing 100190, China

Abstract: Body sensor networks provide a platform for ubiquitous healthcare, driving the diagnosis in hospital static environment to the daily life dynamic context. We realized the importance of sensing of activities, which is not only a dimension of human health but also important context information for diagnosis based on the physiologic data. This paper presents our ubiquitous healthcare system, uCare. It consists of uCare devices and a server system. Currently, the uCare system is designed for cardiovascular disease (CVD) examination and management. The uCare device has been tested in a trial in Beijing Hospital. The uCare system will be further tested in elderly care at home and exercise management in training to measure heart dynamics during training.

Keywords: Body sensor networks; Healthcare applications; Sensor fusion; Ubiquitous healthcare

1 Introduction

There have been a lot of efforts on developing home care and wearable healthcare systems. AlarmNet by Virginia is an example [1] for assisted living and residential monitoring. AlarmNet integrates environmental, physiologic, and activity sensors in a scalable heterogeneous architecture. When talking about context awareness, they typically refer to a context-aware middleware framework [2] to integrate and manage multiple heterogeneous sensor devices in a network environment. Berkeley Tricorder [3] is a wearable health monitoring device capable of measuring a subject's electrocardiogram (ECG), electromyography (EMG), blood oxygenation, respiration (via bioimpedance), and motion. All above works are focused on the platforms either wearable or networked. Few have focused on sensor data fusion and data analysis methods to provide tools for diagnosis in daily life environment.

Here is medical experts' view on the wearable technologies for healthcare [4]: It is demonstrated that the usage of wearable monitoring devices that allow continuous or intermittent monitoring of people in their daily life is critical for the advancement of both the diagnosis and treatment. The usual clinical or hospital monitoring of physiologic events, such as the ECG or blood pressure, has three limitations: 1) they are likely to fail in sampling rare events that may be of profound diagnostic, prognostic, or therapeutic importance; 2) they fail to measure physiologic responses during normal periods of activity, rest, and sleep, which are more realistic indicators of the health of the patient and the patient response to therapeutic intervention; and 3) brief periods of monitoring cannot capture the circadian variation in physiologic signals that appear to reflect the progression of disease. That means, ubiquitous healthcare using body sensor network technologies in daily live context is believed to be the next generation of medical technologies. We started our research on body sensor networks for ubiquitous healthcare from 2004, and developed a three-tier sensor networks system for elderly activity monitoring [5]. What we have learned from our research experiences are as follows:

1) As a research discipline, body sensor networks call for killer applications. Our uCare system is focused on CVD and elderly care because CVD is the number 1 killer of human beings. According to the American Heart Association (AHA) heart disease statistics 2005 update, more than one quarter, or 70,100,000, of Americans suffer from one or more types of CVD. 27,000,000 are estimated to be 65 or older. As the elderly population keeps growing (the worldwide population over 65 is expected to be more than double from 357 million in 1990 to 761 million by 2025), the population suffering from CVD will grow as well. To meet this increasing demand of specialized care for CVD patients, developing personalized home care solution using our proposed body sensor networks is of importance.

2) The basis of ubiquitous healthcare is context-aware data acquisition and analysis. Here, we divide all sensor data into two categories. One is physiologic data, and the other is context data that further consist of subject activity, psychological status, and environment. Context data relate to situation where the physiologic data are captured. The importance of context information must be addressed in healthcare in daily life. The activity types and intensity play very important role. For example, heart rate of 120 per minute is fine if we know the person is running. It is problem if he is sitting quite for sometime already. Context-aware ubiquitous body sensing, context-aware multiple sensor-data fusion, and context-aware diagnosis and therapy will provide basis for healthcare in daily life at home, at work, and on the move, shifting the healthcare emphasis from hospital to home and community, from curing diseases by medical experts to self-care and fitness.

3) Applications call for application-specific hardware and software systems. Therefore, we have moved away from universal sensor node platform, tinyOS, and Zigbee wireless communication. Instead, we choose to develop our own wearable devices for wearability and power efficiency. We adopt Bluetooth because we have to communicate with smart phones in our application.

In the rest of the paper, we first describe the overall architecture of our uCare device and system in Section 2. The ECG processing, activity classification, and the context-aware information fusion are presented in Sections

Received 15 October 2010.

3, 4, and 5, respectively. Section 6 is the conclusion.

2 Architecture

Fig. 1 is the block diagram of the uCare system. A uCare system consists of a server and multiple uCare devices. A uCare device consists of a wearable computer and one or more body sensor nodes. As shown in Fig. 1, there are two categories of sensors: physiologic sensors may include ECG, blood pressure meter, and SpO2, while context sensors may include accelerometers to measure activities, galvanic skin response (GSR) to measure skin conductivity, which related to psychological status, and microphone to measure environment noise level. Sensors are in sensor nodes, which perform data collection, preprocessing, and wireless transmission to the wearable computer. We use smart phone in uCare device as wearable computer. It receives data from sensor nodes via Bluetooth and communicates with the server through Wifi.

Two categories of sensor data are processed in the wearable computer by two modules: vital signal processing and context data processing. For example, ECG data will be first processed to reduce the noise and reform the baseline from disturbances, and then to identify and locate the QRS complex, and finally locate the ST segment. By those processes, heart rate and ECG waveform morphological changes will be evaluated. Meanwhile, activity types are classified and activity intensity is calculated using accelerometer data. Context-based fusion of ECG processing results and activity information will be able to estimate heart status.

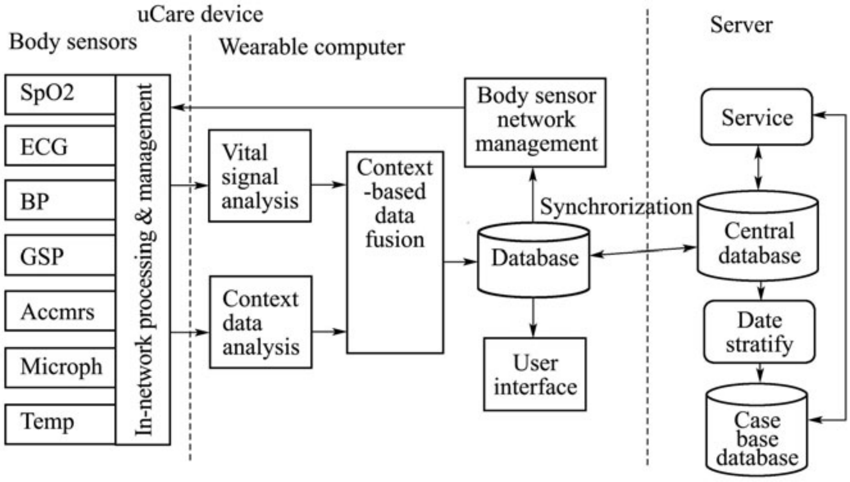

Fig. 1 Block diagram of context-aware healthcare system.

There is a local database in the uCare device and a central database in the server. The local database stores the sensor data and processing results. Abnormalities detected will be accompanied by original ECG waveform, activity information, and time stamp. The local database also stores personal profile of the wearer, the system parameters of sensor nodes, and the settings of the uCare device, for example, warning threshold, warning event definition, etc.

There is a body sensor network management module in the wearable computer, which is a simple version of a middleware to monitor the status of the sensor nodes (shown in Fig. 2). The parameters of those sensor nodes, including sampling rate and communication protocol parameters in the local database, are updated regularly through Bluetooth communication. The sensor nodes will be reset if there is any parameter change in the local database. That change may be the result of interactive function of "setting" by the user or database synchronization with the central database. On other hand, the event of battery level changes will drive the local database update, and consequently the central database update as well. When the battery level reaches the threshold, a warning message will be sent to the user.

Warning on the event of abnormalities is triggered the same way. There is a database entry defining a warning event. The parameters include the name of the abnormality, the function that detects the event, the threshold, the action, the destinations of the message to be sent, and the message and data items to be sent, etc. When the abnormality is detected, or the output of the detection function reaches the threshold, the event is triggered.

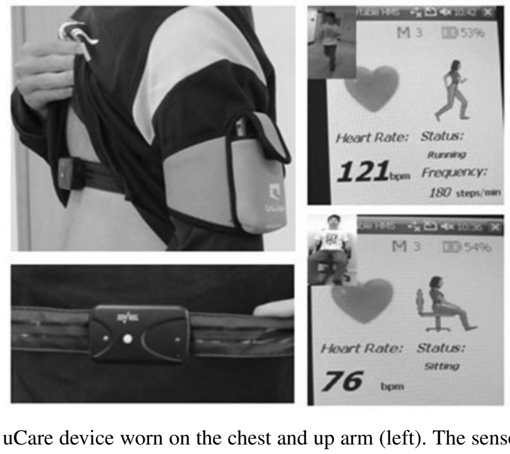

Fig. 2 uCare device worn on the chest and up arm (left). The sensor node has dimension of $56 \times 32 \times 16$ mm and weight of 25 g (bottom left). The smart phone screens (right) show two scenarios of sitting and running, when the heart rate are 76 and 121 bpm, respectively. The running speed is 180 steps per minute.

3 ECG signal processing

ECG carries important information of one's heart status. Many heart diseases can be diagnosed by analyzing ECG waveforms. Computer detection of abnormal beat can automate the cardiovascular disease monitoring. As the basic and crucial step of ECG signal analysis, QRS detection directly affects the accuracy of ECG segmentation and abnormal beat recognition.

3.1 QRS complex detection

There has been a lot of work in ECG signal processing. In reality, the detection ratio, robustness, and time accuracy are important factors in applications. The objectives here are to develop QRS detection algorithm that performs well with respect to all three factors. We make use of the property that symmetric wavelet decomposition can be used to retrieve δ-function-peak location precisely [6]. The coefficients have local maxima at the signal transient points. Digital wavelet transform (DWT) combined with cubic spline interpolation is proposed as a preprocessor. DWT aims to separate baseline drift, QRS complex, and high-frequency noise. The following interpolation is employed to densify the coefficients of each decomposition level. In addition, an improved dynamic weight adjusting strategy is adopted to assign proper weight for each level to further enhance the signal-to-noise ratio (SNR).

The main idea behind this algorithm is that the absolute values of DWT coefficients, generated by decomposing the signal with a symmetric mother wavelet, have local maxima at the signal transient points. How to exploit these local maxima determines the algorithm's performance. Each data segment with length N (N is set to 32) is input consecutively to perform wavelet transform. The coefficients of 3rd, 4th, and 5th levels are preserved because the energy of QRS complex is mainly concentrated on these three levels. The coefficient lengths of them are $N/8$, $N/16$, and $N/32$, respectively, as there is a 2-time down sampling in each decomposition round. The following step interpolates coefficients of these levels with gains of 8, 16, and 32, respectively, to densify the time grid. Then, they each have the same length of N. After that, coefficients of these levels are assigned with periodically updated weights and summed up across levels. After preprocessing step, sequence is passed to a moving integrator,

$$y(n) = \sum_{k=n-N+1}^{n} x(k) \tag{1}$$

to smooth the burrs, where N is set to number of samples in 0.1 second. Finally, a peak detector is employed to generate R peak candidates and an adaptive threshold detector to locate R peaks.

It is known that wavelet coefficient has high time resolution in low decomposition levels and conversely in high decomposition levels. When wavelet coefficients from different levels are summed up, the final time resolution will be aligned to that of the higher level. Therefore, it is reasonable to improve high-level resolution to achieve higher time accuracy. In fact, all these preserved levels are interpolated with different gains. As cubic spline interpolation is a promising technique to evaluate new points between given knots, it is employed in the preprocessing step to densify the wavelet coefficients.

Guaranteeing comparatively high SNR in noise condition is crucial to the robustness of the detector. As mentioned above, different weights are assigned to the interpolated coefficients of the 3rd, 4th, and 5th levels. Each weight can be set to the SNR of that level.

$$w_i = \frac{s_i^2}{n_i^2}, \ \ i = 3, 4, 5. \tag{2}$$

However, the "signal" component and "noise" component cannot be determined precisely, which has a bad influence on retrieving real SNR of each level, especially in heavy noise condition. As the QRS is most relevant to coefficients of level 4, so for other levels, if the weights directly computed from the SNR are larger than a predetermined threshold, it is considered to be unreasonable and reset to a lower value, as in (3). Otherwise, accept the original weights.

$$w_{i\text{new}} = w_i u(th_i - w_i) + th_i u(w_i - th_i), \ \ i = 3, 5, \tag{3}$$

where w_i is the weight of level determined directly from (2), as the threshold, which is an empirical value and is the unit step function.

We tested the algorithm against the MIT-BIH arrhythmia database to evaluate the detecting result. There are 48 half-hour excerpts of two-channel ambulatory ECG recordings, which are digitized at 360 samples per second. In the test, only the first channel, marked "MLII", is used. The statistic results are automatically generated by the evaluator provided by the physionet site.

Tow parameters, sensitivity Se and positive predictivity $+p$, are calculated.

$$Se = \frac{TP}{TP + FN}, \tag{4}$$

$$+p = \frac{TP}{TP + FP}, \tag{5}$$

where TP is the number of true positive detections, FN refers to the number of false-negative detections, and FP stands for false-positive detections. In total, there are 90,989 TP beats, 296 FN beats and 375 FP beats. Therefore, the sensitivity and positive predictivity achieved are 99.68% and 99.59%, respectively. Time accuracy is also taken into account. The total root mean square error turned out to be 15.43 ms.

Test results demonstrated that symmetric wavelet is suited to precisely locate the R peaks in ECG signal. There is a local maximum in the wavelet coefficients at the same time the R peak occurs. How to exploit the local maxima of wavelet coefficients is the key of the algorithms. In this paper, spline interpolation is adopted to improve time resolution of wavelet coefficients in high decomposition levels, which generates smooth curves and suppresses noise to the highest extent. In addition, an improved dynamic weight adjusting strategy is used to improve the SNR in heavy noise condition. Test results have shown the algorithm's robustness and high time accuracy.

3.2 Abnormality detection

The ECG abnormalities uCare can detect now include both abnormal rhythm and premature ventricular contraction (PVC). Rhythm abnormality includes anisorhythmia, tachycardia, bradycardia, pause, and premature beat. Activity of the user is used as context information in arrhythmia detection. In current AHA definition of arrhythmia, abnormal rhythm is only defined when the user is at static status. To follow the AHA definition and detect arrhythmia in daily life, the activity of the subject is checked before starting the arrhythmia detection function. That is, the arrhythmia detection function is triggered only when the subject is in static status (lying, sitting, and standing) for certain time, for example, more than 5 minutes. Study is carried out on arrhythmia detection on the move.

PVC detection process is shown in Fig. 3. The whole algorithm consists of two main steps, namely ECG signal preprocessing and template matching. The preprocessing step is used for baseline wandering removing and signal amplitude normalization to suppress factors that are not related to the type characteristics. In the template matching process, normalized ECG beat waveform is matched against a set of PVC templates, which are preselected to represent PVC variations. To accommodate waveform morphological variations, dynamic time warping (DTW) is used to calculate the distances between the input beat and all templates. The input beat is classified as PVC if the smallest distance with template set is below a threshold.

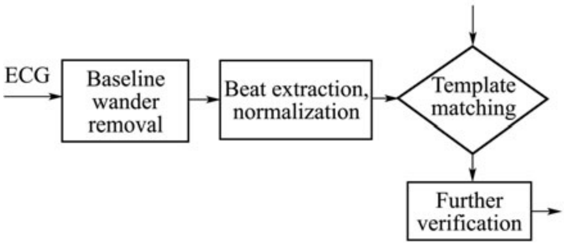

Fig. 3 Diagram of PVC detection process.

Template set selection is critical in the process. The selected templates should well represent all types of PVC waveforms. In the practice, we manually collect as many as possible PVC waveforms. After preprocessing, all PVC waveforms are feed into a clustering algorithm (isodata or k-mean) with DTW distance as the distance measure. After clustering, those cluster centroids are used as templates.

We have tested our algorithm in Beijing Hospital, where we select two patients and let them wear Holter and our uCare device at the same time. The results show that our algorithm has achieved slightly higher PVC detection sensitivity level with the Holter manufactured by a U.S. company currently used in the hospital.

4 Activity classification and quantification

Activity is the most important factor in health monitoring. The uCare system allows options to use 1, 3, 5, or 7 sensor nodes in activity classification and gait analysis. Here, we present activity classification and movement estimation for 1 and 3 sensor nodes cases.

4.1 Activity classification with 1 sensor node

With a triaxial accelerometer attached on the waist, an activity classification method is developed to classify subject's daily physical activities, including lying, sitting, standing, walking, running, and falling. First, energy measure is used to distinguish between static postures and dynamic activities:

$$\begin{cases} E_k = \sum\limits_{i=1}^{N} |a_{k,i} - \bar{a}_k|, \quad k = 1, 2, 3, \\ TE = \sum\limits_{k=1}^{3} E_k, \end{cases}$$

where k stands for the kth axis and N is the sliding window size; here, we chose 2 seconds with 1 second data overlap. $a_{k,i}$ is the ith acceleration data of the kth axis and $\bar{a}_k$ is the average value of the kth axis. Orientation of each axis was used to distinguish among static postures, and walking and running are distinguished using a fixed threshold. Falling is detected by the maximum differential value of vertical acceleration.

Transitions between activity types are also important, and we list some of them as activity types as well. For example, getting up and standing up are critical actions that affect blood circulations and may lead to falls for elderly. Transition probabilities are used to further improve the activity classification accuracy.

4.2 Low limb movement estimation

Low limb movement estimation is crucial in activity and gait analysis. Here, we present low limb movement estimation using 3 accelerometers with our hybrid Bayesian network (HBN). Three accelerometers are attached to waist and thighs as shown in Fig. 4.

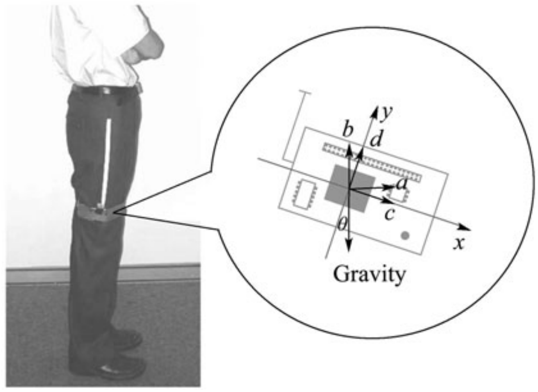

Fig. 4 Placement of the mote and variables of the accelerometer.

Fig. 4 shows the placement of the sensor on the right thigh. In "swing forward" and "swing backward" phases of a gait cycle, the movement of the thigh is stable and the driving force from muscle is comparably small, the system equation can be modeled by constant-angular-velocity model. The average angular velocity can be learnt online and used as a control variable in the state dynamic function, and then the state dynamic function of the system can be written as

$$X_k = AX_{k-1} + Bu + W, \tag{6}$$

where $X_k = [\theta_k \;\; v_k \;\; a_k \;\; b_k]^{\mathrm{T}}$ and $X_{k-1} = [\theta_{k-1} \;\; v_{k-1} \;\; a_{k-1} \;\; b_{k-1}]^{\mathrm{T}}$ are the state variables at time k and $k-1$, respectively. $u = [0 \;\; u_{\mathrm{v}} \;\; 0 \;\; 0]^{\mathrm{T}}$ is the control variable, where u_{v} is the mean angular speed at swing forward or swing backward, K_{v} is a memory factor between 0 and 1.

$$A = \begin{bmatrix} 1 & t_{\mathrm{s}} & 0 & 0 \\ 0 & 1-K_{\mathrm{v}} & 0 & 0 \\ 0 & 0 & 1 & 0 \\ 0 & 0 & 0 & 1 \end{bmatrix} \text{ and } B = \begin{bmatrix} 1 & 0 & 0 & 0 \\ 0 & K_{\mathrm{v}} & 0 & 0 \\ 0 & 0 & 1 & 0 \\ 0 & 0 & 0 & 1 \end{bmatrix} \text{ are}$$

the state transition matrix and control matrix, respectively, where t_{s} is the sampling interval. In equation (6), $W = [w_\theta \;\; w_{\mathrm{v}} \;\; w_{\mathrm{a}} \;\; w_{\mathrm{b}}]^{\mathrm{T}}$ is the system noise. w_θ, w_{v}, w_{a}, and w_{b} are noise of the respective state variables. Although W is non-Gaussian distribution and can be approximated by mixture Gaussian distributions, here we only consider the most significant component and assume W to be independent, zero mean Gaussian noise with distribution given below:

$$P(w_\theta, w_{\mathrm{v}}, w_{\mathrm{a}}, w_{\mathrm{b}}) \sim N(0, Q), \tag{7}$$

where

$$Q = \begin{bmatrix} Q_\theta & 0 & 0 & 0 \\ 0 & Q_{\mathrm{v}} & 0 & 0 \\ 0 & 0 & Q_{\mathrm{a}} & 0 \\ 0 & 0 & 0 & Q_{\mathrm{b}} \end{bmatrix}. \tag{8}$$

Q_θ, Q_v, Q_a, Q_b are variance of the respective state variables. During the "heel off" and "heel strike" phases, however, the state variables may change abruptly due to the sudden strike or forward force and will not obey the linear system equation in (6) anymore. To overcome the problem, we adopt approach in [7] by bringing in control variables $u = [u_\theta \;\; u_\mathrm{v} \;\; 0 \;\; 0]^\mathrm{T}$, where u_θ, u_v is the mean vector of joint probability density function for hip angle and angular velocity in "heel off" phase or "heel strike" phase, and then the state dynamic equation can be written as

$$X_k = AX_{k-1} + Bu + W, \tag{9}$$

where

$$A = \begin{bmatrix} 1-K_\theta & t_\mathrm{s} & 0 & 0 \\ 0 & 1-K_\mathrm{v} & 0 & 0 \\ 0 & 0 & 1 & 0 \\ 0 & 0 & 0 & 1 \end{bmatrix}, \quad B = \begin{bmatrix} K_\theta & 0 & 0 & 0 \\ 0 & K_\mathrm{v} & 0 & 0 \\ 0 & 0 & 1 & 0 \\ 0 & 0 & 0 & 1 \end{bmatrix}.$$

K_θ and K_v are memory factors between 0 and 1. Other variables have the same meaning as in equation (6).

For simplicity, we assume that the measurement equation keeps the same form but with different noise levels in all phases of a gait cycle. The relationship between the measured accelerations c, d and the state variables are as

$$\begin{cases} c_k = g\sin\theta_k + a_k\cos\theta_k - b_k\sin\theta_k + w_\mathrm{c}, \\ d_k = -g\cos\theta_k + a_k\sin\theta_k + b_k\cos\theta_k - rv_k^2 + w_\mathrm{d}, \end{cases} \tag{10}$$

or in matrix form,

$$Y_k = h(X_k) + V, \tag{11}$$

where $Y_k = [c_k \;\; d_k]^\mathrm{T}$ is the measurement vector, and $V = [w_\mathrm{c} \;\; w_\mathrm{d}]^\mathrm{T}$ is measurement noise. As the same reason for system noise W, V is also assumed to be independent, zero-mean Gaussian noise, i.e.,

$$P(w_\mathrm{c}, w_\mathrm{d}) \sim N(0, R), \tag{12}$$

where $R = \begin{bmatrix} R_\mathrm{c} & 0 \\ 0 & R_\mathrm{d} \end{bmatrix}$ is the covariance matrix.

In order to represent phases of gait cycle, we use hybrid dynamic Bayesian network as depicted in Fig. 5 and described by the following set of state-space equations:

$$S_t \sim p(S_t|S_{t-1}), \tag{13}$$

$$X_t = A(S_t)X_{t-1} + B(S_t)u + W(S_t), \tag{14}$$

$$Y_t = h(X_t) + V(S_t), \tag{15}$$

where $S_t \in \{1, 2, 3, 4\}$ denotes the four phases of a gait cycle. Because S_t plays the role of switching, when $S_t \in \{1, 3\}$, it indicates that thigh movement is the "heel off" or "heel strike" phase, equation (13) will be the same as equation (9); when $S_t \in \{2, 4\}$, $B(S_t)$ is the control matrix that affects the angular velocity, and equation (13) takes the form of equation (6).

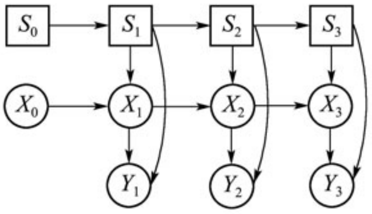

Fig. 5 Hybrid dynamic Bayesian network representation of the system model, square nodes are discrete and round nodes are continuous. S denotes instances of the gait cycle phase with continuous valued state X and observation Y.

In order to evaluate the hip angle, we usually evaluate the maximum a posterior (MAP) distribution $p(X_{0:t}|Y_{0:t})$. This distribution can be derived from the posterior distribution $p(S_{0:t}, X_{0:t}|Y_{0:t})$ by standard marginalization, where (S, X) is denoted as hybrid state. The posterior density satisfies the following recursion:

$$\begin{aligned} &p(S_{0:t}, X_{0:t}|Y_{0:t}) \\ &\quad = p(S_{0:t-1}, X_{0:t-1}|Y_{0:t-1}) \\ &\qquad \times \frac{p(Y_t|X_t, S_t)p(X_t, S_t|X_{t-1}, S_{t-1})}{p(Y_t, Y_{1:t-1})}. \end{aligned} \tag{16}$$

Unfortunately, this recursion is not trackable. Therefore, we resort to sequential Monte Carlo method (particle filter) to approximate the posterior distribution, and the experimental results is shown in Figs. 6 and 7 [8]. It is important to note that for each realization of S_t, the probability density function of X_t can be approximated by a Gaussian distribution using the extended Kalman filter or unscented Kalman filter effectively.

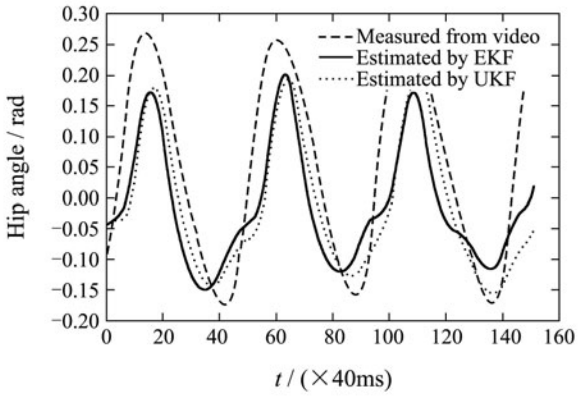

Fig. 6 Hip angle tracking result using Kalmen filter.

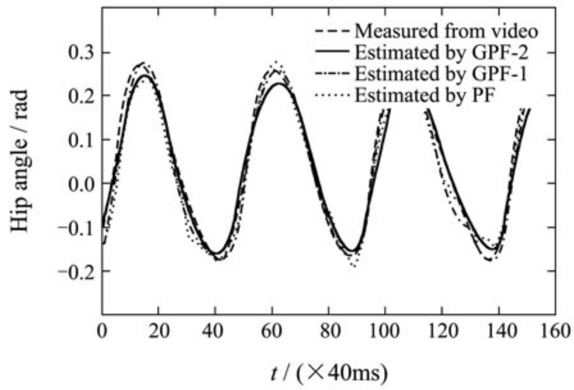

Fig. 7 Hip angle tracking result using hybrid dynamic Bayesian network.

5 Fusion of vital signal and context information

Fig. 8 shows the Bayesian network for the fusion of vital signal and context information to reason for heart status. The heart status H is a hidden state, while ECG is the measurement, where heart rate R and ECG waveform morphology M can be derived. Activity A and temperature T are two causal factors that affect the heart status. The posterior probability of the heart status can be calculated as follows:

$$p(H|R, M, A, T) = \frac{p(R, M|H, A, T)p(H)}{p(R, M|A, T)}. \tag{17}$$

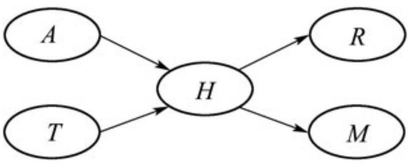

Fig. 8 Bayesian network for context-aware data fusion.

Here, activity A takes values of $\{$lie down, sitting, standing, walking, running slowly, running fast, upstairs, downstair$\}$. The temperature T takes values of $\{$hot, warm, cool, cold$\}$. The heart status H is represented by cardiovascular fitness and takes five states $\{$Excellent, Good, Fair, Poor, Very Poor$\}$. From the formula, we can see that the evaluation of one's cardiovascular fitness requires calculation of two likelihood functions of $p(R, M|H, A, T)$ and $p(R, M|A, T)$ and the probability $p(H)$. We have entered into a project on the study of heart dynamics during the training (HDDT) using uCare devices. After collection of ECG and activity type, intensity, and duration data, we are able to derive these probabilities and then to obtain the norms given the probability of heart status $p(H)$.

Fig. 9 shows the system screen dump of fusion of heart rate and activities, where the heart rate, activity type, and motion intensity are plotted along the time line to help the doctor to learn about the heart rate dynamics. This may help the doctor to find rules and abnormal heart rate changes during the user's dynamic status.

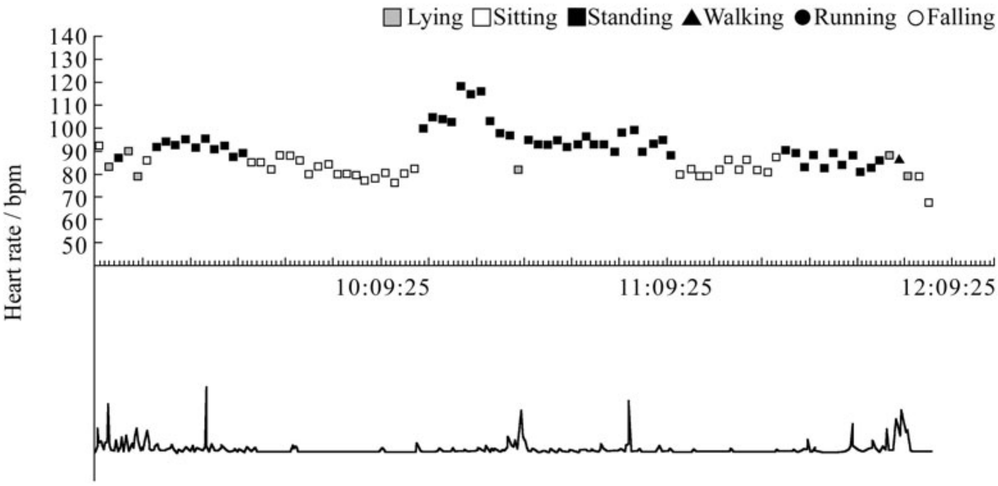

Fig. 9 System screen dump of fusion of heart rate and activities.

6 Conclusions

We have presented a body sensor network for ubiquitous healthcare application, uCare system, and discussed the details regarding architecture, the real-time activity classification, ECG signal processing, and context-aware data fusion. The beta product has passed the first round trial.

Acknowledgements

The authors acknowledge the previous and current members of the research center who have contributed to the projects and further development, especially, Dr. Zhiqiang Zhang and Huabin Zheng.

References

[1] A. Wood, J. Stankovic, G. Virone, et al. Context-aware wireless sensor networks for assisted living and residential monitoring[J]. *IEEE Network*, 2008, 22(4): 26 – 33.

[2] A. Esposito, L. Tarricone, M. Zappatore, et al. A framework for context-aware home-health monitoring[J]. *International Journal of Autonomous and Adaptive Communications Systems*, 2010, 3(1): 75 – 91.

[3] R. Naima, J. Canny. The Berkeley tricorder: Ambulatory health monitoring[C]//*Proceedings of the 6th International Workshop on Wearable and Implantable Body Sensor Networks*. Los Alamitos: IEEE Computer Society, 2009: 53 – 58.

[4] P. Binkley, W. Frontera, D. Standaert, et al. Predicting the potential of wearable technology: Physicians share their vision of future clinical applications of wearable technology[J]. *IEEE Engineering in Medicine and Biology Magazine*, 2003, 22(3): 23 – 27.

[5] J. Wu, S. Bao, D. Cheng, et al. Sensor augmented aging in place[C]//*IEEE International Workshop on Biomedical Circuits & Systems*. Singapore, 2004: 13 – 16.

[6] H. Zheng, J. Wu. Real-time QRS detection method[C]//*The 10th IEEE International Conference on e-Health Networking, Applications and Services*. New York: IEEE, 2008: 169 – 170.

[7] Z. Zhang, J. Wu, Z. Huang. Gaussian particle filter for tracking hip angle in gait cycles[C]//*The 10th IEEE International Conference on e-Health Networking, Applications and Services*. New York: IEEE, 2008: 177 – 181.

[8] L. Dong, J. Wu, X. Chen. Real-time physical activity monitoring by data fusion in body sensor networks[C]//*Proceedings of the 10th International Conference on Information Fusion*. New York: IEEE, 2007: 1576 – 1582.

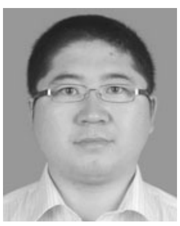

Shaofeng WANG received his B.S. degree in Software Engineering from Nankai University, China. He is currently a M.S. student of Electrical Engineering at the Graduate University, Chinese Academy of Sciences. Currently, he is working at the Sensor Networks and Application Joint Research Center, Graduate University and Institute of Automation, Chinese Academy of Sciences. His research interests focus on dynamic ECG signal processing under various activity intensities and new applications on body sensor network. E-mail: wang123sf@gmail.com.

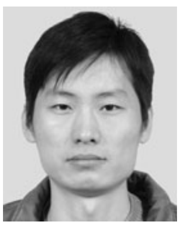

Lianying JI received his B.S. degree in Communication Engineering from Dalian Maritime University, Dalian, China, and Ph.D. in Signal and Information Processing from Beijing Institute of Technology, Beijing, China. Since 2009, he work as a postdoctoral fellow in Sensor Network Application and Research Center of Chinese Academy of Sciences. His research interests include ELINT systems and body sensor network. E-mail: jiliany-ing@gmail.com.

Aiguang LI received his B.E. degree in Electronic Engineering from the Beijing Institute of Technology, Beijing, China, in 2008. Currently, he is pursuing his M.E. degree of Computer Sciences Engineering at the Graduate University, Chinese Academy of Sciences. His research interests focus on body sensor networks for patient monitoring and biomedical signal processing. E-mail: aiguang.li@gmail.com.

Jiankang WU received his B.S. from University of Science and Technology of China, and Ph.D. from Tokyo University. He is currently a professor at the Graduate University, Chinese Academy of Sciences. He is directing the Sensor Networks and Applications Research Center (SNARC), which is jointly operated by the Graduate University and Institute of Automation, Chinese Academy of Sciences. Prior to his current position, he was Principal Scientist and Department Manager of New Initiatives Department at the Institute for Infocomm Research (I2R), Singapore (known as Kent Ridge Digital Labs (KRDL) in 1998-2001 and Institute of System Science (ISS) before 1998). He created new research initiatives in the areas of NeuroInformatics and PhysioInformatics, embedded sensor network systems in I2R, and led a series of large international collaborative projects in KRDL and ISS. He was a full-time professor in University of Science and Technology of China (USTC) until 1993, where he received 9 distinguished awards from the nation and Chinese Academy of Sciences. He has also worked in universities in U.S., U.K., Germany, France, and Japan.

Dr. Wu pioneered several researches in the area of visual information processing, including adaptive image coding in later 70s, object-oriented GIS in early 80s, face recognition technology in 1992, content-based multimedia indexing and retrieval in 90s, and rights management for multimedia contents in later 90s. He initiated and led 3 large international collaborative labs. He was regarded as "an exceptionally bright visionary" by U.S. Giga Information Group. He is an author of 18 patents, more than 100 papers and 5 books. E-mail: jkwu@gucas.ac.cn.